

This item is the archived peer-reviewed author-version of:

Plasma streamer propagation in structured catalysts

Reference:

Zhang Quan-Zhi, Bogaerts Annemie.- Plasma streamer propagation in structured catalysts
Plasma sources science and technology / Institute of Physics [Londen] - ISSN 0963-0252 - 27:10(2018), 105013
Full text (Publisher's DOI): <https://doi.org/10.1088/1361-6595/AAE430>
To cite this reference: <https://hdl.handle.net/10067/1555100151162165141>

Plasma streamer propagation in structured catalysts

Quan-Zhi Zhang^{*}, Annemie Bogaerts

Research Group PLASMANT, University of Antwerp, Universiteitsplein 1, B-2610 Antwerp-Wilrijk, Belgium

E-mail: Quan-Zhi.Zhang@uantwerpen.be

Abstract

Plasma catalysis is gaining increasing interest for various environmental applications. Catalytic material can be inserted in different shapes in the plasma, e.g., as pellets, (coated) beads, but also as honeycomb monolith and 3DFD structures, also called “structured catalysts”, which have high mass and heat transfer properties. In this work, we examine the streamer discharge propagation and the interaction between plasma and catalysts, inside the channels of such structured catalysts, by means of a two-dimensional particle-in-cell/Monte Carlo collision model. Our results reveal that plasma streamers behave differently in various structured catalysts. In case of a honeycomb structure, the streamers are limited to only one channel, with low or high plasma density when the channels are parallel or perpendicular to the electrodes, respectively. In contrast, in case of a 3DFD structure, the streamers can distribute to different channels, causing discharge enhancement due to surface charging on the dielectric walls of the structured catalyst, and especially giving rise to a broader plasma distribution. The latter should be beneficial for plasma catalysis applications, as it allows a larger catalyst surface area to be exposed to the plasma.

Keywords: Plasma catalysis, streamer propagation, 3D structures, PIC/MCC

1. Introduction

Plasma catalysis is of interest for various environmental applications, such as gaseous pollutant removal and greenhouse gas conversion, as it combines the advantages of high reactivity from plasma technology with selectivity from catalysis [1-6]. The interactions between plasma and catalytic material often yield synergetic effects, resulting in enhanced efficiency of chemical processes. Studying plasma discharges in narrow channels of various supporting dielectric materials and heterogeneous catalysts is of great importance, as it defines the active surface area of the catalyst exposed to plasma. Many types of catalytic material and shapes can be applied, including spheres (packed bed), foams, honeycombs, three dimensional fibre deposition (3DFD) structure, including so-called 1-1, 1-3, and 1-3-5 stacking architecture [7]. This notation refers to the position of the fibres with respect to each other, as explained in section 2.

In general, the structure of the supporting/catalytic material is of crucial importance for the chemical processes [7]. Compared to packed beds with spheres, so-called structured catalysts, like honeycombs and 3DFD structures, have the advantages of higher mass and heat transfer, and lower pressure drop, which has been demonstrated to yield a higher conversion rate in converting methanol to olefins under the same operation conditions in thermal catalysis [7].

Plasma discharges in honeycomb catalysts have already been investigated experimentally, because these structures allow a large surface area with low pressure drop for improved chemical reactions [8-12]. However, it is difficult to generate a homogenous and stable electrical discharge inside a honeycomb structure [13]. Kirkpatrick et al. thus proposed a two-stage reactor that consists of a plasma reactor with a honeycomb structure catalyst located downstream of the plasma [14]. To allow gas ionization and plasma formation inside the fine channels of a honeycomb catalyst, Hensel et al. presented a novel approach of a sliding discharge, which is the superposition of an AC barrier discharge inside a catalytic pellet bed, coupled in series with a DC powered honeycomb monolith [8-11]. The discharge starts from the AC packed bed, and then slides into the channels of the honeycomb

monolith, and generates a homogenous discharge, under the effect of the DC electric field. Furthermore, instead of using a packed bed discharge, Hensel et al. also introduced a diffuse coplanar surface barrier discharge as auxiliary discharge [15]. A strong surface discharge takes place on the dielectric barrier, with high number density of charged particles, which provide a sufficient amount of seeds for initiating a homogenous honeycomb discharge. Furthermore, Kang et al. applied a plasma discharge in a honeycomb structured catalyst for automobile exhaust treatment, by a hybrid DBD reactor with a 2 mm gap between the high voltage electrode and honeycomb catalyst [16]. The plasma is generated in the gap and then develops into the honeycomb monoliths. The authors verified that an effective synergistic effect of plasma and catalyst was achieved, and the automobile exhaust gas can be well decomposed.

A few papers have reported the discharge behavior in a dielectric capillary tube, which can mimic a honeycomb structure, by numerical modeling [17, 18]. By means of a fluid model, Jánský' et al. presented simulations of air discharge propagation at atmospheric pressure initiated by a needle anode in a dielectric capillary tube [17]. They studied the influence of the radius of the tube and its relative permittivity on the discharge behavior. For fixed relative permittivity of 1, the discharge was found to be homogeneous, and could fill the tube during its propagation, at a tube radius of 0.1 mm. When increasing the radius to 0.3-0.6 mm, the discharge structure became tubular with peak values of electric field and electron density close to the dielectric surface. Further enlarging the tube radius (above 0.7 mm) had no influence on the discharge behavior. For fixed tube radius, the discharge structure gradually became tubular when increasing the relative permittivity from 1 to 10. In addition, the discharge velocity increased with the decrease in both the tube radius and relative permittivity. In a follow-up paper, Jánský' et al. further indicated, by a combination of experiments and simulations, that the maximum velocity of the discharge propagation appeared in a tube with radius slightly less than 100 μm , and that the discharge velocity in the tubes increased linearly with the applied voltage [18]. Hence, these authors simulated the discharge dynamics in a honeycomb-like structure by a single capillary tube, by changing the tube radius and relative permittivity, but the interaction between plasma and catalyst (or catalyst support), e.g., surface charging, which influences the discharge behavior, was not examined. In the present work, we simulate the streamer propagation initiated from different locations inside a honeycomb monolith channel, and we study the interaction between plasma and catalyst support (i.e. surface charging), by means of a particle-in-cell/Monte Carlo collision (PIC/MCC) model. This model can explicitly track the charged particles in the discharge and can reveal more physical details (like streamer branching), compared to a fluid model. In addition, we will compare the discharge structure for a honeycomb monolith channel with other structured catalysts.

As the diameter of the honeycomb monolith channel is normally small (0.1~2 mm), in all the above papers, the monolith channels are set perpendicular to the electrodes to allow the discharge to propagate over a long distance, and thus to obtain sufficient plasma density. Only a few papers [19, 20] studied honeycomb monolith packed bed discharges (where the honeycomb monolith channels are parallel to the electrodes), in which the emphasis was not put on the catalyst support structure, but the influence of the gas flow and electrical parameters on toluene decomposition and carbon dioxide reforming was investigated. Despite quite some efforts have been devoted to the feasibility of realizing plasma catalysis in a honeycomb catalyst, the plasma discharge mechanism and interaction between plasma and catalyst still remain very poorly understood.

In addition, although 3DFD structures were demonstrated to exhibit higher methanol-to-olefin conversion in thermal catalysis, compared to a packed bed with spheres and a honeycomb type structure [7], there are no investigations yet on plasma discharge formation in 3DFD structured catalysts. Especially the streamer propagation mechanism in different structured catalysts is not clear, which is very important for the optimization of specific plasma catalysis applications.

In the present work, we therefore investigate the streamer discharge propagation in different structured catalysts, including honeycombs, 3DFD 1-1, 3DFD 1-3 and 3DFD 1-3-5 stacking architecture. For this

purpose, we use a 2D implicit PIC/MCC model. We will compare the influence of the catalyst (support) structure on the discharge evolution, and estimate the corresponding performance of plasma catalysis.

Note that when writing “catalyst structure”, we actually refer to the “catalyst support structure”. Indeed, in the present model, we only account for the support structure, which is in mm scale, and we don’t consider the characteristic features of the catalyst, typically dispersed as nanoparticles on the support, such as surface area, porosity, surface conductivity, and the presence of active metals. These features may also play an important role in the plasma propagation and catalytic performance. However, adding these characteristics would require multi-scale simulations (ranging from mm for the reactor and support scale, to nm for the catalytic nanoparticles and pore sizes). Indeed, we would need to use a grid size in the nm scale, and the latter is not compatible with the mm dimensions of the reactor, as it would yield $\sim 10^6$ (in one direction) grid points (keeping in mind the uniform mesh structure in our current model), resulting in excessive computation times and computer memory. In addition, taking into account the catalytic surface area would require a 3D model, which would again lead to excessive computation times and computer memory in the PIC/MCC simulations. Hence, accounting for these catalytic features is beyond the scope of our PIC/MCC model. However, in our previous work, we investigated plasma streamer propagation in porous catalysts [21, 22], so the combination of both types of simulations gives a more comprehensive picture of plasma catalysis.

2. Simulation geometry

In the simulation, the catalysts are put in the gap (4.2 mm) between two electrodes, which are covered by dielectric plates with thickness of 0.3 mm (bottom) and 0.5 mm (top), and relative permittivity $\epsilon_r = 4$. The bottom electrode is powered by a negative DC voltage, while the top electrode is grounded.

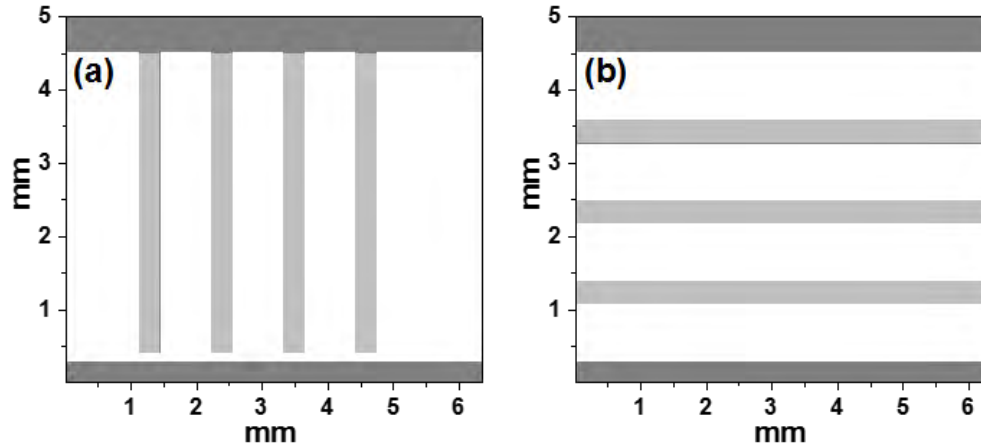


Figure 1. Schematic of the simulation geometry of a plasma reactor with honeycomb monolith (in light grey), with the channels perpendicular (a) and parallel (b) to the electrodes. The electrodes are at the top and bottom of the figure, and they are covered by dielectric plates (in dark grey), with thickness of 0.3 mm (bottom) and 0.5 mm (top).

Since the channel sidewalls in a honeycomb monolith are all closed, we can define a 2D simulated honeycomb monolith discharge geometry as in figure 1. The channels can be set perpendicular to the electrodes (figure 1a), or parallel to the electrodes (figure 1b). The discharge develops in the separated channels, which are rectangular with a size of 0.8×0.8 mm. The thickness of the channel sidewalls is 0.32 mm.

The structures of the 3DFD catalysts are constructed by stacking fibres layer by layer, parallel to the electrodes. Figure 2 presents the top view, side view and simulation geometry of the 3DFD 1-1 stacking structure. In the side view of figure 2(b), the light grey fibres are perpendicular to the plane, hence parallel to the electrodes. The four grey fibres shown in figure 2(a) correspond to the four grey

fibres in one plane parallel to the electrodes in figure 2(b,c). This 1-1 stacking architecture has straight channels in both the vertical direction (i.e., perpendicular to the electrodes), with a size of 0.8×0.8 mm (as seen from the top view in figure 2a), and horizontal direction (i.e., parallel to the electrodes), with a size of 0.32×0.32 mm (as seen from the side view in figure 2b). The thickness of the fibres is again 0.32 mm. As the applied electric field is between the electrodes from the side view (figure 2b), the plasma streamer will develop in the straight channels perpendicular to the electrodes. We can thus simulate the plasma discharge by a 2D model in the direction of streamer propagation, i.e. we simulate a cross section of the structure from the bottom electrode to the top electrode, cutting the cross section along the dashed line from the top view in figure 2(a) (perpendicular to the plane shown in figure 2a). Note that this cross section corresponds to the side view in figure 2(b), but in between the blue fibres. As the latter are thus not involved in the simulated cross section, we can remove them from figure 2(b), and we achieve the simulation geometry in figure 2(c), with only the grey fibres of figure 2(b).

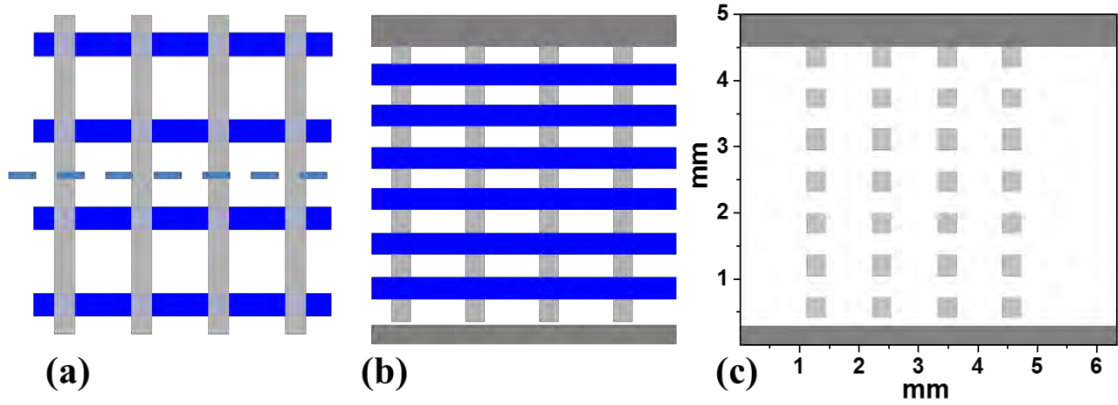


Figure 2. Top view (a), side view (b) and simulation geometry (c), of the 3DFD 1-1 stacking structure. In (a) the upper and lower electrode and dielectrics are not drawn for the sake of clarity. The dashed line in (a) indicates the simulation cross section perpendicular to the plane. The fibres are in blue and light grey colour, and the dielectric plates covering the electrodes are in dark grey colour. The light grey fibres are perpendicular to the plane in (b,c).

We also investigate two modified 3DFD architectures, with the fibres shifted a bit at different layers, i.e. 3DFD 1-3 stacking and 3DFD 1-3-5 stacking [7]. Figure 3 shows their top views and side views. In the 1-3 stacking architecture, the fibres of the upper layer are all shifted $1/2$ of the ‘gap’ (between two fibres in the same layer) relative to the fibres in the adjacent layer below, while in the 1-3-5 stacking architecture, the fibres of the upper layer are all shifted $1/3$ of the ‘gap’ relative to the fibres in the adjacent layer below. Note that here, we only shift the grey fibres for clarity to construct the architectures, as we only include the grey fibres in our simulation. In practice, the blue fibres can also be shifted to construct different architectures. Again we simulate a 2D cross section as indicated by the dashed line in figure 3(a, b), which corresponds to the side views of figure 3(c, d). Again, the blue fibres will be removed to get the simulation geometries in figure 4.

Figure 4 shows the resulting simulation geometries of the 3DFD 1-3 and 1-3-5 stacking architectures, with only the grey fibres kept. The simulated architecture now consists of many curved channels, which may induce significant differences in the streamer propagation.

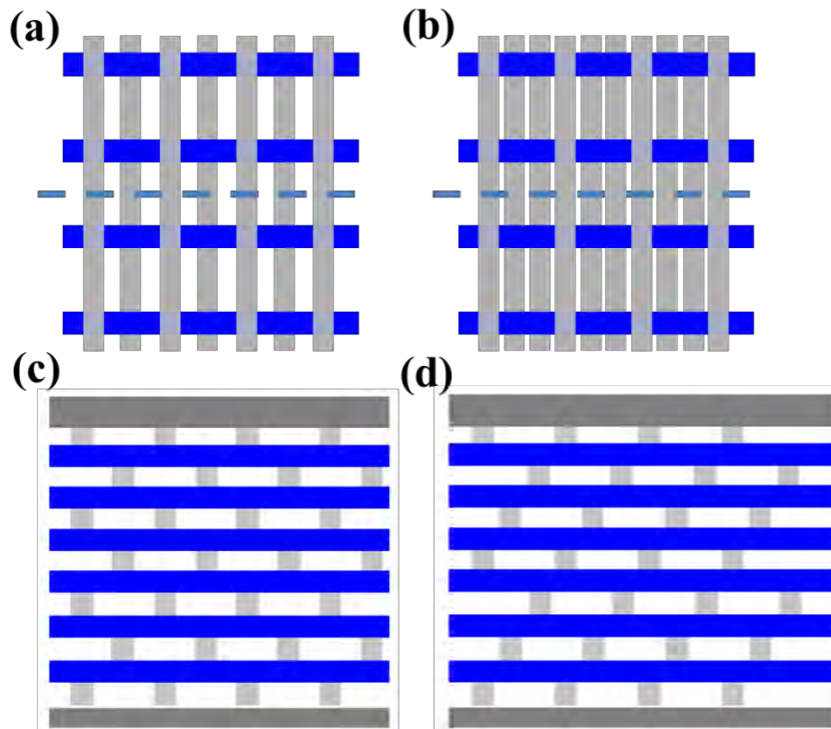


Figure 3. Top views (a, b), and side views (c, d), of the 3DFD 1-3 (a,c) and 3DFD 1-3-5 (b,d) stacking structure. In (a, b) the upper and lower electrode and dielectrics are not drawn for the sake of clarity. The dashed line in (a, b) indicates the simulation cross section perpendicular to the plane. The fibres are in blue and light grey colour, and the dielectric plates covering the electrodes are in dark grey colour. The light grey fibres are perpendicular to the plane in (c,d).

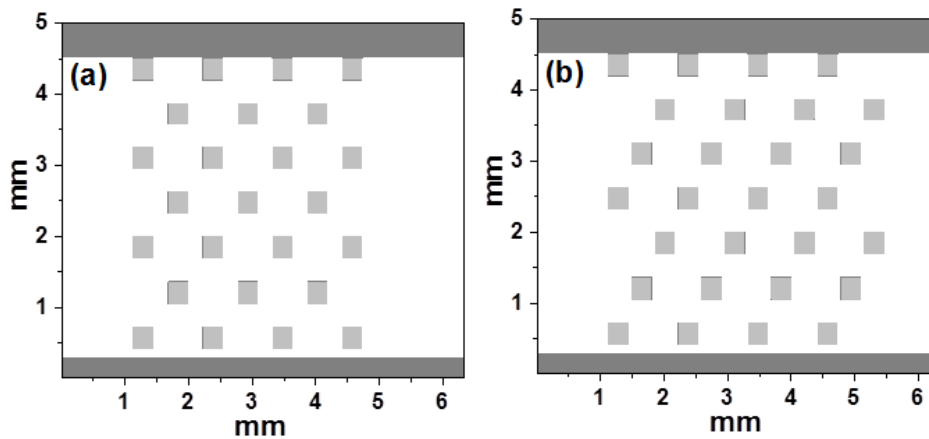


Figure 4. Simulation geometries of the 3DFD 1-3 (a), and 3DFD 1-3-5 (b) stacking structure. The electrodes are at the top and bottom of the figure, and they are covered by dielectric plates (in dark grey). The light grey fibres are perpendicular to the plane.

Note that there is a very small gap between the bottom electrode and the structured catalysts in figure 1(a), figure 2(c) and figure 4, which is needed for locating the seed particles in the model, in order to artificially initiate the discharge. Indeed, in practical plasma catalysis with honeycomb structure catalysts, the plasma is generally ignited outside of the honeycomb structure, and it will slide into the structured catalysts, acting as seeds for initiating a discharge inside the structure under the effect of an applied electric field [8-11, 15, 16]. This corresponds to the seed particles in our model, in which a negative DC voltage is used to force the seed particles (mainly electrons) into the structured catalysts and ignite the plasma streamer.

Note that we only consider a negative DC voltage (i.e., negative streamer) in our simulations, to be consistent with the experiments of Refs [8-11, 15], and because modelling a positive streamer is more challenging in terms of computer memory and computation time, due to the development of many branches.

Note that in each geometry, we only consider the dielectric constant of the catalyst support structure, assuming it to be a catalytic support with dielectric constant of SiO₂ ($\epsilon_r=4$), and we don't look at chemical surface effects.

3. Computational Model

We apply a 2D implicit PIC/MCC model, for which a detailed description can be found in [23, 24]. We follow the behavior of the following plasma species: electrons, O₂⁻, O₂⁺, and N₂⁺ ions. They are represented by so-called super-particles, which correspond to a certain number of real particles, as defined by their weight [25]. The streamer is initiated by artificially placing 20 seed super-particles of each species (electrons, O₂⁻, O₂⁺, and N₂⁺ ions) right above the bottom dielectric, with initial weight ω_p equal to 1 (i.e., 1 super-particle corresponds to 1 electron or ion). The number of real particles will increase with the streamer discharge evolution, because more ions and electrons are created upon ionization avalanches in the gas. To account for this, and at the same time to restrict the computation time, the weight of the super-particles will automatically increase by the particle merging algorithm, i.e. when the number of each kind of super-particle exceeds 50 in a grid, three particles are combined into two particles with both conservation of energy and momentum.

Although in reality there will be more than one streamer developed in the discharge, especially in a configuration with needles-plate electrode with needle gap larger than 1 mm [26], the streamers would all behave very similarly. This is indeed illustrated in figure A1 in the Appendix, showing a simulation result for two separate streamers in two adjacent channels. Therefore, and in order to limit the computation time and to avoid the risk of exceeding the computer memory when simultaneously simulating multiple streamers, we have only set one bunch of seed particles in the model to simulate the evolution of a single streamer, following also other PIC/MCC simulations of streamer evolution [27-30].

The initial velocities of super-particles are sampled from a Maxwellian distribution with average energy of 2 eV for the electrons and 0.026 eV for the ions. The electrons and ions will accumulate on the dielectric surface of the catalyst (support) structure and the dielectric plate at the top dielectric, and thus contribute to surface charging of the adjacent grids on the dielectric surface, when arriving at these dielectric surfaces. Square simulation cells are used in the model. The simulation region is uniformly divided into 1024 × 1300 cells, with a mesh size around 5 μm for all the geometries investigated. The simulation time-step is fixed at 10⁻¹² s. A negative DC voltage of -20 kV is applied at the bottom electrode, while the top electrode is grounded. Thus, an initial electric field of 4×10⁶ V/m is applied throughout the gap in the DBD.

Dry air at 300 K and 1 atm is considered as the discharge gas, with a constant density of background molecules (O₂, N₂). Free electrons, N₂⁺, O₂⁺ and O₂⁻ are traced during the whole simulation. The collisions taken into account are elastic, excitation, ionization and attachment collisions of electrons with O₂ and N₂ gas molecules, as explained in more detail in [29]. All the collision cross sections are adopted from the LXcat database [31]. We employ the stochastic version of Zheleznyak's photoionization model [27, 28, 30, 32, 33] to account for photoionization, i.e. ionization of O₂ molecules after absorbing photons emitted by excited N₂ molecules, with a wavelength between 98 and 102.5 nm. The model directly calculates the number and location of photoionization events, which is originally built based on experimental measurements. Note that the number and movement of photons are not explicitly treated in this model. Good agreement has been achieved for this model with

experimental measurement in [32]. This photoionization model is also widely adopted in other PIC/MCC simulations [27, 28, 30, 33].

4. Results and discussion

4.1 Honeycomb monolith structure

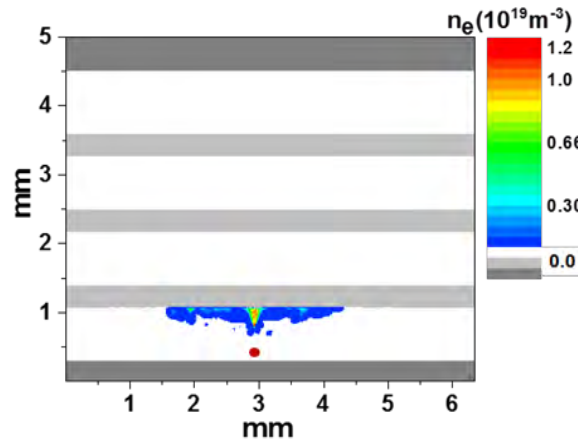


Figure 5. Plasma density distributions n_e (m^{-3}), at 0.8 ns, illustrating the evolution of a plasma streamer in a honeycomb monolith structure with the channels parallel to the electrodes. The red spot indicates the location of the seed particles. Both the dielectric plates covering the electrodes and the support material are in dark grey colour, and the same applies to the figures below).

Figure 5 illustrates the plasma streamer propagation in a honeycomb monolith structure with the channels parallel to the electrodes. The red spot in the figure shows the location of the seed particles (idem in the figures below, i.e. the red spot always shows the location of the seed particles). A certain distance is needed for the generation of a plasma streamer from the avalanche of the seed particles. The streamer first arrives at the dielectric, and then develops along the dielectric surface, yielding a surface discharge. The local maxima at the surface indicate discharge enhancements, caused by photoionization. However, as the plasma streamer can only develop within the short diameter (~ 0.8 mm) of one channel, the plasma density is quite low, i.e. in the order of 10^{19} m^{-3} . This will give rise to limited production of reactive plasma species upon electron impact reactions, and it may explain why in practice the channels are mostly perpendicular to the electrodes in plasma catalysis applications with honeycomb structured catalysts [8-11, 15, 16].

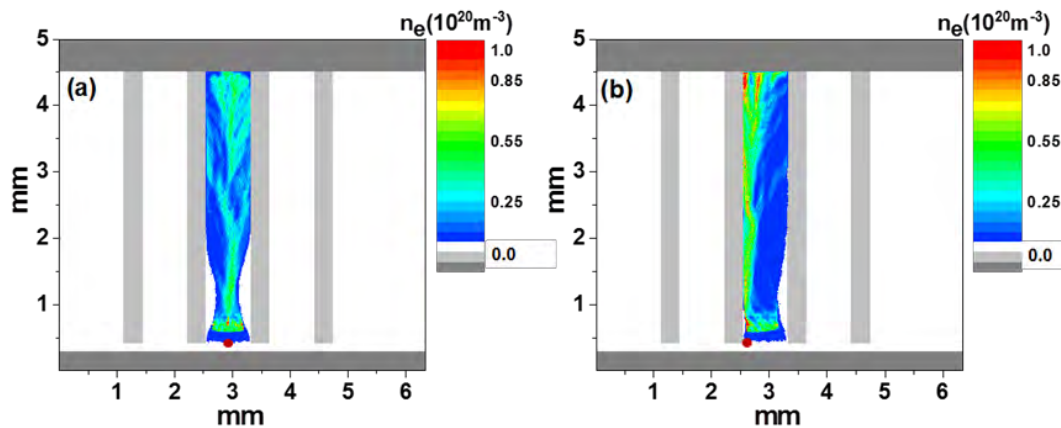


Figure 6. Plasma density distributions n_e (m^{-3}), at 1.12 ns, illustrating the evolution of a plasma streamer in a honeycomb monolith structure with the channels perpendicular to the electrodes, for two different locations of streamer initiation (see red spot): (a) at the centre of the channel, (b) along the dielectric of the honeycomb structure.

In figure 6, we show the plasma streamer propagation in a honeycomb monolith structure with the channels perpendicular to the electrodes. The seed particles are located either in the centre of the channel (a), or close to the channel sidewall (b). The streamer discharge is obviously limited to a single channel, indicating that the streamers in different channels of a honeycomb structured catalyst are completely separated.

Compared to figure 5, the plasma density is an order of magnitude higher in figure 6, as the plasma streamer can develop over a much longer distance. This qualitatively correlates with experimental observations [15], where the measured emission intensity (which should roughly be proportional to the plasma density) gradually increases till a saturation value upon larger distance from the negative DC biased electrode.

In addition, the discharge is much more enhanced in figure 6(b), i.e., when it is initiated along the dielectric surface of the honeycomb structure. Indeed, when the plasma streamer develops, the charged particles (mainly electrons due to their small mass) will charge the dielectric surface. The charging will be non-uniform as a function of propagation distance. The accumulated electrons on the dielectric surface will further induce an electric field along the surface. This electric field will further push the electrons in the direction of streamer propagation, i.e., this induced electric field is in the same direction as the applied electric field. The total electric field is thus enhanced, yielding a higher plasma density. We reported a similar enhancement effect due to dielectric surface charging for plasma streamer propagation inside catalyst pores [22].

We can conclude that the plasma discharge is more pronounced when the honeycomb channels are perpendicular to the electrodes. In addition, the position of streamer initiation also largely affects the plasma density. In practical application, the position of streamer initiation can be controlled to some extent by using a needle electrode (with opposite plane electrode), as demonstrated in the experiments of [34].

Note that all calculations presented in this paper were performed with dielectric barriers covering both electrodes, because this yielded more stable calculations. Indeed, when a streamer arrives at the metallic electrode, the plasma density near the electrode will sharply increase (just like an unstable localized spark in experiments). This may render the simulations unstable, because the particle numbers increase rapidly. Thus, to prevent this ‘spark transition’, we assumed dielectric barriers covering the electrodes. However, it should be noted that the same streamer behavior in the channels is predicted without dielectric barriers at the electrodes (see figure A2 in the Appendix).

4.2 3DFD 1-1 stacking architecture

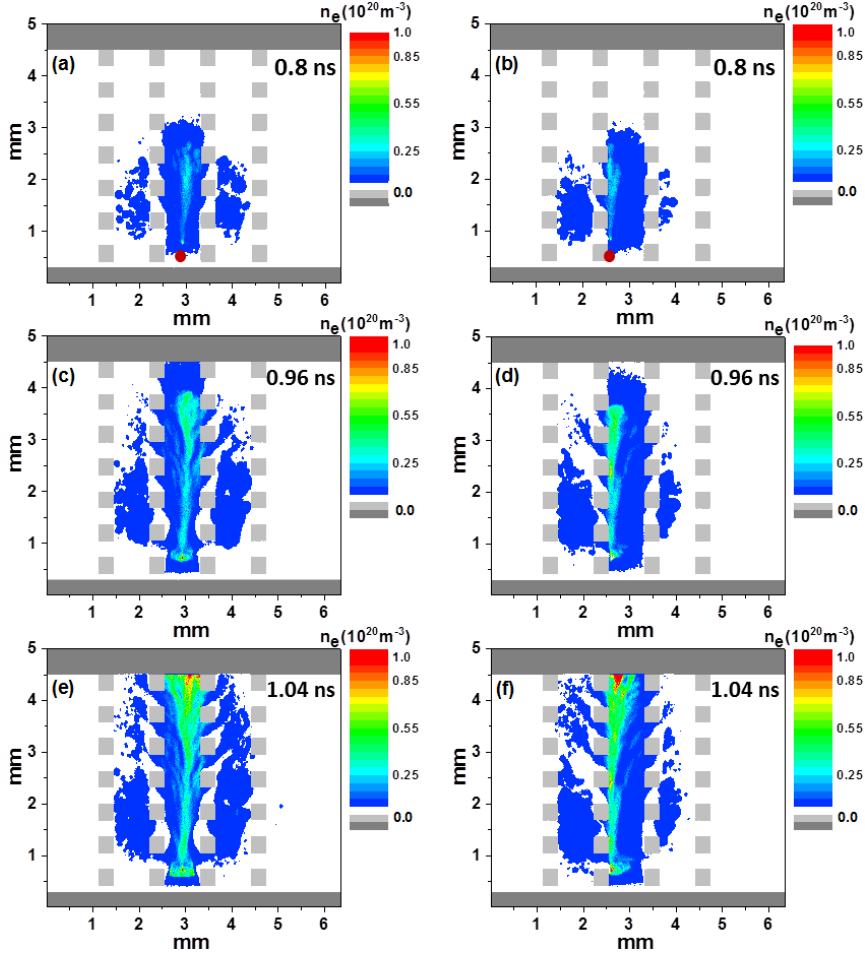


Figure 7. Plasma density distributions n_e (m^{-3}), at 0.8 ns (a)-(b), 0.96 ns (c)-(d), 1.04 ns (e)-(f) (when the streamers reach the top dielectric), illustrating the evolution of a plasma streamer in a 3DFD 1-1 stacking architecture, for two different locations of streamer initiation (see red dot in (a)-(b)): (a), (c), (e) streamer initiation at the centre of the channel; (b), (d), (f) streamer initiation along the dielectric of the 3DFD structure.

Figure 7 presents the plasma density distributions for two different locations of the seed particles in a 3DFD 1-1 stacking architecture. While the maximum plasma density is comparable to the results for the honeycomb structure (figure 6), the plasma distribution becomes much broader. Indeed, the plasma can spread into other channels through the gap between the dielectric layers, which gives rise to a streamer with many small branches, whereas in the honeycomb structure the plasma was limited to one channel. Moreover, photoionization can happen directly in the other channels, and contribute to further streamer enhancement.

4.3 3DFD 1-3 stacking architecture

Figure 8 presents the plasma density distributions for two different locations of the seed particles in a 3DFD 1-3 stacking architecture. When the streamer initiates at the centre of the channel (figure 8a), the middle dielectric splits the streamer into two streamers. Since the new streamers further develop toward the top electrode under a certain angle, they are further split into more streamers when they arrive at the other dielectric walls of the 3DFD structure. In contrast, when the streamer starts along the dielectric (figure 8b), it can get in touch with the dielectric at both the left and right sides of its path, resulting in some enhancement due to surface charging. The enhanced streamer gradually becomes wider and is further split into more streamers by the dielectric walls of the 3DFD structure closer to the top electrode.

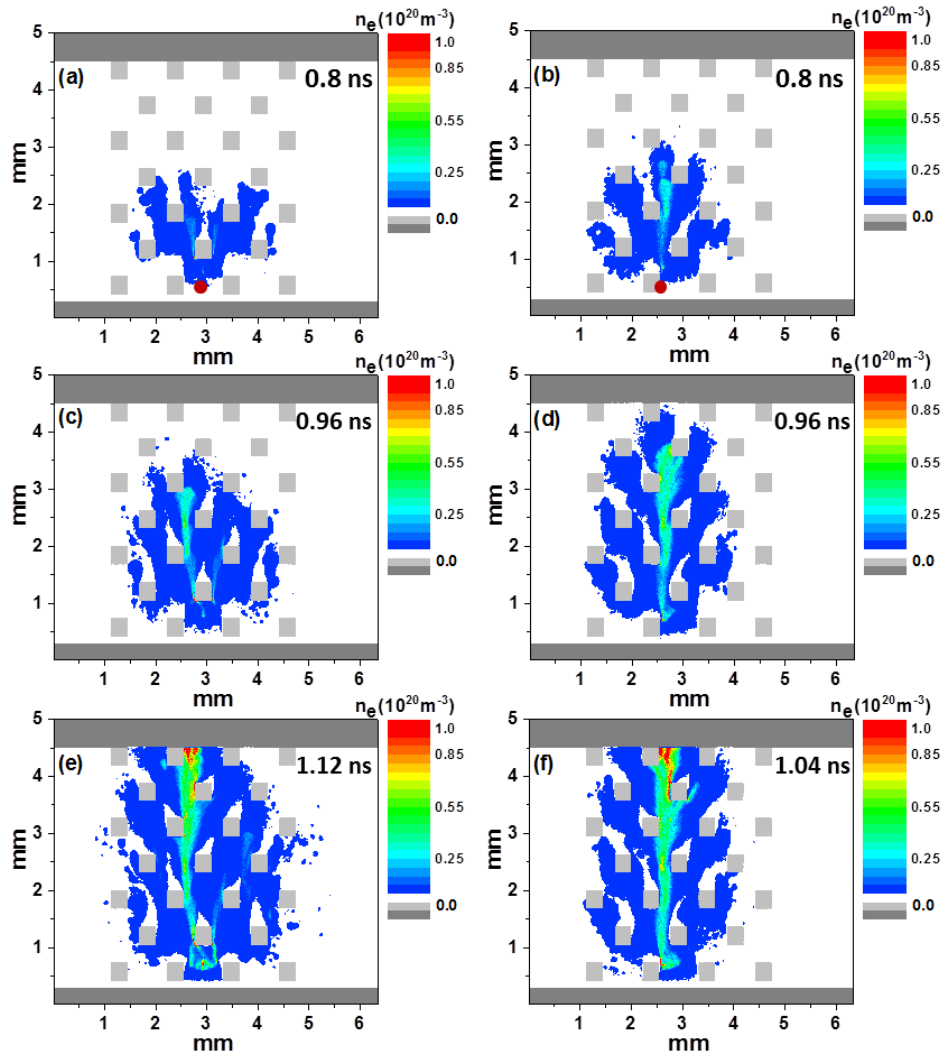


Figure 8. Plasma density distributions n_e (m^{-3}), at 0.8 ns (a)-(b), 0.96 ns (c)-(d), 1.12 ns (e) and 1.04 ns (f) (when the streamers reach the top dielectric), illustrating the evolution of a plasma streamer in a 3DFD 1-3 stacking architecture, for two different locations of streamer initiation (see red dot in (a)-(b)): (a), (c), (e) at the centre of the channel; (b), (d), (f) along the dielectric of the 3DFD structure.

4.4 3DFD 1-3-5 stacking architecture

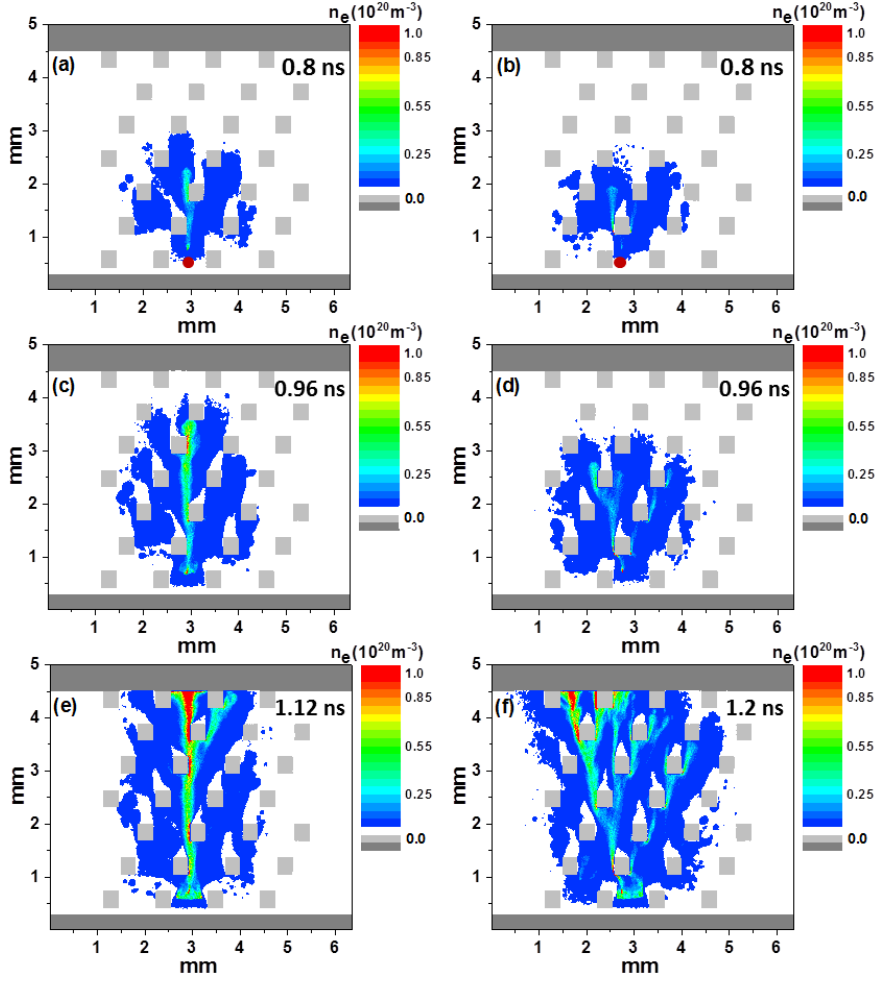


Figure 9. Plasma density distributions n_e (m^{-3}), at 0.8 ns (a)-(b), 0.96 ns (c)-(d), 1.12 ns (e) and 1.2 ns (f) (when the streamers reach the top dielectric), illustrating the evolution of a plasma streamer in a 3DFD 1-3-5 stacking architecture, for three different locations of streamer initiation (see red dot in (a)-(b)): (a), (c), (e) at the centre of the channel; (b), (d), (f) at 1/4 of the channel gap.

Finally, the plasma density distribution for the 3DFD 1-3-5 stacking architecture are plotted in figure 9. When the streamer initiates from the centre of the channel (figure 9a), as the distance between subsequent layers in the 3DFD structure is quite small, the streamer can charge the dielectric walls of the structure at different layers, and contribute to significant discharge enhancement.

When the streamer initiates from 1/4 of the channel gap (figure 9b), i.e. right below the second layer dielectric, the streamer is first split into two streamers, and when it arrives at the next dielectric layer, it will charge the bottom of that dielectric layer, which generates a horizontal surface electric field and promotes the streamer development in the lateral direction. In combination with the effect of the vertical applied electric field, the streamers develop a parabolic path. The streamers will arrive at the dielectrics in the next layer, and this behavior is repeated layer by layer. The same actually happens in figure 9 (a, c, e), when the streamer becomes wide enough to be split by the dielectric structures closer to the top electrode. During this parabolic path, the streamer induces many small discharge enhancements on the further dielectric surfaces of the 3DFD structure, yielding many small streamers, which result in a much broader discharge area. This will improve the discharge homogeneity, and give rise to a larger catalyst surface area exposed to plasma, which is expected to enhance the utilization of the catalytic material.

Again, we believe that the position of streamer initiation, and thus corresponding discharge distributions and enhancements, can be somewhat controlled by applying a needle electrode, but this should be further investigated experimentally.

From the time evolution of the streamer presented in figures 7-9 above, we roughly estimate the average streamer propagation speed to be about $3\text{-}4\times 10^6$ m/s, depending on the catalyst support structure and the position of streamer initiation. These propagation speeds are comparable to the experimental values for gas-phase streamers, reported by Briels et al. in air discharge [35], with comparable electric field intensity, i.e. in the order of 10^6 V/m. Indeed, these authors reported a streamer propagation speed around 4×10^6 m/s for 100 kV applied voltage over a 4 cm gap. These propagation speeds are a bit higher than in a typical packed-bed DBD [36, 37], where values around 5×10^5 m/s were calculated for a comparable electric field in the order of 10^6 V/m. This can be explained by the fact that the packing beads/pellets distort the propagation paths of the streamers, while the structured catalyst supports in this work have a large free volume to allow fast streamer propagation, just like for gas-phase streamers without packing. We can also see from figures 7-9 that the streamer propagation speed increases with time, from around 2.0×10^6 m/s at 0.8 ns to around 6.0×10^6 m/s at 0.96 ns. This agrees well with the calculation results in [37], where the streamer speed was around 2.3×10^5 m/s before reaching the central discharge region, and it became 5×10^5 m/s before reaching the top discharge region. Besides, as indicated in the experiments of [36], there are normally many streamer branches in a packed-bed DBD along the gap between the beads/pellets (for small dielectric constant of 5). However, as seen from figures 7, 8, and 9, the branching of plasma streamers in this work largely depends on the catalyst support structure and the position of streamer initiation. The branches in the gas-phase plasma streamers in [35] are somewhat random, hence similar to the honeycomb monolith (as seen in figure 6(a-b)). In addition, the calculated electron density and the electric field in the structured catalyst supports studied in this work are all in the same order as in typical packed-bed DBD [36, 37], i.e. 10^{20} m⁻³ and 10^6 V/m, respectively.

It is worth to mention that although photoionization is less important for negative streamer propagation than for positive streamer propagation, it still has some effect in the case of negative streamer propagation as well, i.e., it broadens the plasma distribution and accelerates the streamer propagation a bit. This can be seen by comparing figures 6(a) and 9(e) (obtained with photoionization) with figures A3(a,b) in the Appendix, showing the calculated electron density profiles in the case of streamer propagation in a honeycomb structure and a 3DFD 1-3-5 stacking architecture without photoionization. Nevertheless, the photoionization rate is much lower than the electron impact ionization rate, as also indicated in [29, 37]. Since the photoionization does not really change the character of the streamer propagation, we do not go in further detail on the photoionization effect in this work.

5. Conclusions

In this work, we studied the plasma streamer propagation mechanism in different structured catalysts by means of a PIC-MCC model in dry air. Our simulation results reveal that in case of a honeycomb structure, the plasma discharge is limited in a single channel, and that the discharge is quite weak when the honeycomb channels are parallel to the electrodes, because the streamer can develop only over a short distance. In contrast, when the honeycomb channels are perpendicular to the electrodes, the plasma density is an order of magnitude higher, as the streamer can develop over a much longer distance within the channels. Especially when the streamer is initiated along the dielectric surface, the discharge will be further enhanced due to surface charging along the dielectric surface.

In a 3DFD structure, the streamers can develop into other channels, through the gaps between the different dielectric layers of the 3DFD structure. Surface charging of the dielectrics enhances the discharge. Furthermore, the location of streamer initiation also induces significant differences in the streamer distributions.

A 3DFD structure with 1-3-5 architecture has curved channels, and exhibits either more enhanced plasma streamers or a much broader discharge area, depending on the location of streamer initiation. This broader discharge area allows a larger catalyst surface area to be exposed to the plasma, which will improve the performance of plasma catalysis.

These results are highly interesting for practical applications. We believe that the position of streamer initiation can be controlled by a needle electrode, generating the desired plasma streamer distribution as predicted by our model, but this will need to be investigated experimentally.

In real experiments, the catalyst support structures can be further improved by optimizing the fibre thickness and the spacing between the fibres/sidewalls, to reach a higher performance in plasma catalysis. Besides, as the evolution mechanisms of positive plasma streamers are very different from negative streamers, it is also interesting to investigate the interaction between positive plasma streamers and catalyst supports. We thus plan to investigate the geometry (thickness and spacing) optimization of catalyst support structures, as well as the propagation of positive streamers in structured catalysts in our future work. Finally, our current simulations only consider the catalyst support structure, and not the catalyst itself, which is typically dispersed as (transition metal or metal oxide) nanoparticles on the support. The characteristic features of this catalyst, such as surface area, porosity and surface conductivity, might also affect the streamer propagation. Taking this into account in our PIC/MCC simulations is very challenging, as it requires a 3D model (to account for the surface area) and multi-scale simulations (ranging from mm for the reactor and support structures to nm for the catalyst nanoparticles and pores). Nevertheless, in our future work we would like to investigate these effects, to bring the simulations closer to the application.

Acknowledgments

We acknowledge financial support from the European Marie Skłodowska-Curie Individual Fellowship within H2020 (Grant Agreement 702604). This work was carried out in part using the Turing HPC infrastructure at the CalcUA core facility of the Universiteit Antwerpen, a division of the Flemish Supercomputer Center VSC, funded by the Hercules Foundation, the Flemish Government (department EWI) and the University of Antwerp.

Appendix

Separate plasma streamers develop in two channels at the same time

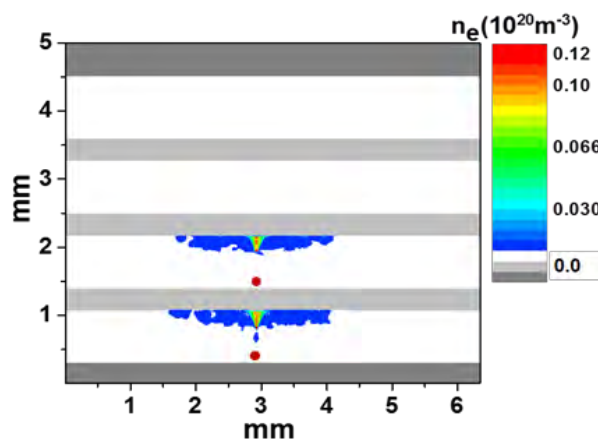


Figure A1. Plasma density distributions, at 0.8 ns, illustrating the evolution of a plasma streamer in a honeycomb monolith structure with channels parallel to the electrodes. Two separate bunches of seed particles are placed in the first and second channel, respectively.

Figure A1 shows the calculation results for separate streamers in separate channels of the honeycomb structure, by setting two separate bunches of seed particles. As can be seen, the streamers develop separately from each bunch of seed particles, and behave very similarly.

Plasma streamer propagation without dielectric barriers near the electrodes

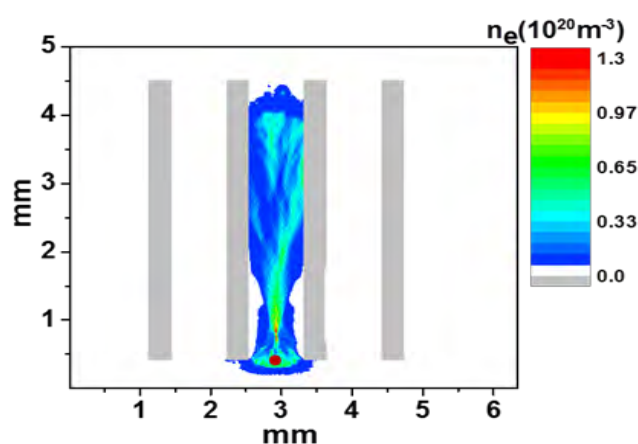


Figure A2. Plasma density distributions, illustrating the evolution of a plasma streamer in a honeycomb monolith structure, without dielectric barriers near the electrodes.

As can be seen by comparing figure A2 and figure 6(a), when the dielectrics are removed, the streamers behave very similarly in the channel (before arriving at the electrode). As the effective voltage applied on the catalyst is increased due to removing the dielectrics, the plasma density increases a bit in figure A2.

Photoionization effect in negative streamer propagation

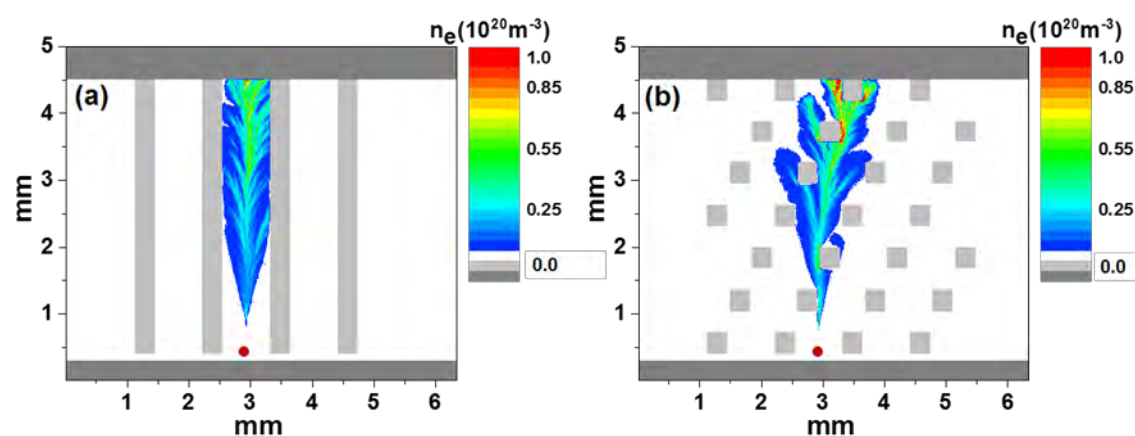


Figure A3. Plasma density distributions n_e (m^{-3}), illustrating the evolution of a plasma streamer in (a) a honeycomb monolith structure at 1.28 ns, and (b) a 3DFD 1-3-5 stacking architecture at 1.28 ns, without photoionization.

Figure A3 shows the plasma streamer propagation without photoionization. By comparing figure 6(a) and figure 9(e) (obtained with photoionization) with figures A3(a, b), we can easily see that the photoionization broadens the plasma distribution and accelerates the streamer propagation a bit. However, since the maximum plasma density remains almost the same when including the photoionization, we can conclude that the photoionization rate is much lower than the electron impact ionization rate, as also indicated in [29, 37].

[1] E. C. Neyts, K. K. Ostrikov, M. K. Sunkara, et al. Plasma Catalysis: Synergistic Effects at the Nanoscale. *Chemical Reviews*. 2015, 115(24):13408–13446. <https://doi.org/10.1021/acs.chemrev.5b00362>

[2] H.-H. Kim, A. Ogata, S. Futamura. Oxygen Partial Pressure-dependent Behavior of Various Catalysts for the Total Oxidation of Voc's Using Cycled System of Adsorption and Oxygen Plasma.

- Applied Catalysis B: Environmental. 2008, 79(4):356 – 367. <http://www.sciencedirect.com/science/article/pii/S0926337307003864>
- [3] J. V. Durme, J. Dewulf, C. Leys, et al. Combining Non-thermal Plasma with Heterogeneous Catalysis in Waste Gas Treatment: A Review. Applied Catalysis B: Environmental. 2008, 78(3):324 – 333. <http://www.sciencedirect.com/science/article/pii/S0926337307003037>
- [4] H. L. Chen, H. M. Lee, S. H. Chen, et al. Review of Plasma Catalysis on Hydrocarbon Reforming for Hydrogen Production - Interaction, Integration, and Prospects. Applied Catalysis B: Environmental. 2008, 85(1):1 – 9. <http://www.sciencedirect.com/science/article/pii/S0926337308002403>
- [5] J. C. Whitehead. Plasma Catalysis: The Known Knowns, the Known Unknowns and the Unknown Unknowns. Journal of Physics D: Applied Physics. 2016, 49(24):243001. <http://stacks.iop.org/0022-3727/49/i=24/a=243001>
- [6] E. C. Neyts, A. Bogaerts. Understanding Plasma Catalysis Through Modelling and Simulation - a Review. Journal of Physics D: Applied Physics. 2014, 47(22):224010. <http://stacks.iop.org/0022-3727/47/i=22/a=224010>
- [7] J. Lefevre, M. Gysen, S. Mullens, et al. The Benefit of Design of Support Architectures for Zeolite Coated Structured Catalysts for Methanol-to-olefin Conversion. Catalysis Today. 2013, 216:18 – 23. <http://www.sciencedirect.com/science/article/pii/S0920586113002903>
- [8] K. Hensel, S. Sato, A. Mizuno. Electrical Discharge in Honeycomb Monolith. Chemické Listy. 2008, 102:S1318–S1321
- [9] S. Sato, K. Hensel, H. Hayashi, et al. Honeycomb Discharge for Diesel Exhaust Cleaning. Journal of Electrostatics. 2009, 67(2):77 – 83. <http://www.sciencedirect.com/science/article/pii/S0304388609000965>
- [10] K. Hensel, S. Sato, A. Mizuno. Sliding Discharge Inside Glass Capillaries. IEEE Transactions on Plasma Science. 2008, 36(4):1282–1283
- [11] K. Hensel. Microdischarges in Ceramic Foams and Honeycombs. The European Physical Journal D. 2009, 54(2):141. <https://doi.org/10.1140/epjd/e2009-00073-1>
- [12] A. Mizuno. Generation of Non-thermal Plasma Combined with Catalysts and Their Application in Environmental Technology. Catalysis Today. 2013, 211:2 – 8. <http://www.sciencedirect.com/science/article/pii/S0920586113001314>
- [13] T. Yamamoto, M. Okubo, T. Kuroki, et al. Nonthermal Plasma Regeneration of Diesel Particulate Filter. Tech. rep., SAE Technical Paper, 2003
- [14] M. J. Kirkpatrick, E. Odic, J.-P. Leininger, et al. Plasma Assisted Heterogeneous Catalytic Oxidation of Carbon Monoxide and Unburned Hydrocarbons: Laboratory-scale Investigations. Applied Catalysis B: Environmental. 2011, 106(1):160 – 166. <http://www.sciencedirect.com/science/article/pii/S0926337311002281>
- [15] J. R. K. Hensel, M. Janda. Generation of Discharges Inside the Honeycomb Monolith Assisted by Diffuse Coplanar Surface Barrier Discharge. 19th International Symposium on Plasma Chemistry. Bochum, Germany, 2009
- [16] W. S. Kang, D. H. Lee, J.-O. Lee, et al. Combination of Plasma with a Honeycomb-structured Catalyst for Automobile Exhaust Treatment. Environmental science & technology. 2013, 47(19):11358–11362

- [17] J. Jansky, F. Tholin, Z. Bonaventura, et al. Simulation of the Discharge Propagation in a Capillary Tube in Air at Atmospheric Pressure. *Journal of Physics D: Applied Physics*. 2010, 43(39):395201. <http://stacks.iop.org/0022-3727/43/i=39/a=395201>
- [18] J. Jansky, P. L. Delliou, F. Tholin, et al. Experimental and Numerical Study of the Propagation of a Discharge in a Capillary Tube in Air at Atmospheric Pressure. *Journal of Physics D: Applied Physics*. 2011, 44(33):335201. <http://stacks.iop.org/0022-3727/44/i=33/a=335201>
- [19] T. Kuroki, T. Fujioka, M. Okubo, et al. Toluene Concentration Using Honeycomb Nonthermal Plasma Desorption. *Thin solid films*. 2007, 515(9):4272–4277
- [20] V. Goujard, J.-M. Tatibouet, C. Batiot-Dupeyrat. Influence of the Plasma Power Supply Nature on the Plasma–catalyst Synergism for the Carbon Dioxide Reforming of Methane. *IEEE Transactions on Plasma Science*. 2009, 37(12):2342–2346
- [21] Q.-Z. Zhang, A. Bogaerts. Propagation of a Plasma Streamer in Catalyst Pores. *Plasma Sources Science and Technology*. 2018, 27(3):035009. <http://stacks.iop.org/0963-0252/27/i=3/a=035009>
- [22] Q.-Z. Zhang, W.-Z. Wang, A. Bogaerts. Importance of Surface Charging During Plasma Streamer Propagation in Catalyst Pores. *Plasma Sources Science and Technology*. 2018, 27(6):065009. <http://stacks.iop.org/0963-0252/27/i=6/a=065009>
- [23] H. Yu Wang, W. Jiang, Y. Nian Wang. Implicit and Electrostatic Particle-in-cell/monte Carlo Model in Two-dimensional and Axisymmetric Geometry: I. Analysis of Numerical Techniques. *Plasma Sources Science and Technology*. 2010, 19(4):045023. <http://stacks.iop.org/0963-0252/19/i=4/a=045023>
- [24] W. Jiang, H. Yu Wang, Z. Hua Bi, et al. Implicit and Electrostatic Particle-in-cell/monte Carlo Model in Two-dimensional and Axisymmetric Geometry: II. Self-bias Voltage Effects in Capacitively Coupled Plasmas. *Plasma Sources Science and Technology*. 2011, 20(3):035013. <http://stacks.iop.org/0963-0252/20/i=3/a=035013>
- [25] C. K. Birdsall. Particle-in-cell Charged-particle Simulations, Plus Monte Carlo Collisions with Neutral Atoms, Pic-mcc. *IEEE Transactions on Plasma Science*. 1991, 19(2):65–85
- [26] H. Ueno, S. Kawahara, H. Nakayama. Influence of Needle Tip Distance on Barrier Discharge and Ozone Generation for Multiple Needle-and-plane Electrode Configuration. *Electronics and Communications in Japan*. 93(7):32–41. <https://onlinelibrary.wiley.com/doi/pdf/10.1002/ecj.10289>, <https://onlinelibrary.wiley.com/doi/abs/10.1002/ecj.10289>
- [27] L. Ningyu, P. V. P. Effects of Photoionization on Propagation and Branching of Positive and Negative Streamers in Sprites. *Journal of Geophysical Research: Space Physics*. 2004, 109(A4). <https://agupubs.onlinelibrary.wiley.com/doi/pdf/10.1029/2003JA010064>, <https://agupubs.onlinelibrary.wiley.com/doi/abs/10.1029/2003JA010064>
- [28] J. Teunissen, U. Ebert. 3d Pic-mcc Simulations of Discharge Inception Around a Sharp Anode in Nitrogen/oxygen Mixtures. *Plasma Sources Science and Technology*. 2016, 25(4):044005. <http://stacks.iop.org/0963-0252/25/i=4/a=044005>
- [29] Y. Zhang, H. Yu Wang, Y. Ru Zhang, et al. Formation of Microdischarges Inside a Mesoporous Catalyst in Dielectric Barrier Discharge Plasmas. *Plasma Sources Science and Technology*. 2017, 26(5):054002. <http://stacks.iop.org/0963-0252/26/i=5/a=054002>

- [30] O. Chanrion, T. Neubert. A Pic-mcc Code for Simulation of Streamer Propagation in Air. *Journal of Computational Physics*. 2008, 227(15):7222 – 7245. <http://www.sciencedirect.com/science/article/pii/S0021999108002210>
- [31] Biagi-v8.9 Database. Accessed: 11 June, 2015, www.lxcat.net
- [32] M. A. K. Zheleznyak M B, S. S. V. Teplofiz. *Vys. Temp.* 1982, 20:423–8
- [33] Y. Li, R. Wang, Q. Zhang, et al. Particle-in-cell/monte Carlo Simulation of Positive Streamers with Photoionization Model. *IEEE Transactions on Plasma Science*. 2011, 39(11):2226–2227
- [34] M. J. Z. M. J. Zigo, K. Hensel. Discharge Propagation in Honeycomb Monolith. 5th Central European Symposium on Plasma Chemistry (CESPC). Balaton, Hungary, 2013:128–129
- [35] T. M. P. Briels, J. Kos, G. J. J. Winands, et al. Positive and Negative Streamers in Ambient Air: Measuring Diameter, Velocity and Dissipated Energy. *Journal of Physics D: Applied Physics*. 2008, 41(23):234004. <http://stacks.iop.org/0022-3727/41/i=23/a=234004>
- [36] W. Wang, H.-H. Kim, K. V. Laer, et al. Streamer Propagation in a Packed Bed Plasma Reactor for Plasma Catalysis Applications. *Chemical Engineering Journal*. 2018, 334:2467 – 2479. <http://www.sciencedirect.com/science/article/pii/S1385894717320612>
- [37] J. Kruszelnicki, K. W. Engeling, J. E. Foster, et al. Propagation of Negative Electrical Discharges Through 2-dimensional Packed Bed Reactors. *Journal of Physics D: Applied Physics*. 2017, 50(2):025203. <http://stacks.iop.org/0022-3727/50/i=2/a=025203>